

13. Patel, N., Dadhwal, V. and Saha, S., Measurement and scaling of carbon dioxide (CO₂) exchanges in wheat using flux-tower and remote sensing. *J. Indian Soc. Remote Sensing*, 2011, **39**, 383–391.
14. Patil, M. *et al.*, Measurements of carbon dioxide and heat fluxes during monsoon-2011 season over rural site of India by eddy covariance technique. *J. Earth Syst. Sci.*, 2014, **123**, 177–185.
15. Watham, T. *et al.*, Monitoring of carbon dioxide and water vapour exchange over a young mixed forest plantation using eddy covariance technique. *Curr. Sci.*, 2014, **107**, 858–867.
16. Anderson, B. E. *et al.*, Airborne observations of spatial and temporal variability of tropospheric carbon dioxide. *J. Geophys. Res.: Atmos.*, 1996, **101**, 1985–1997.
17. Machida, T. *et al.*, Worldwide measurements of atmospheric CO₂ and other trace gas species using commercial airlines. *J. Atmos. Ocean. Technol.*, 2013, **25**, 1744–1754.
18. Chen, H. *et al.*, High-accuracy continuous airborne measurements of greenhouse gases (CO₂ and CH₄) using the cavity ring-down spectroscopy (CRDS) technique. *Atmos. Meas. Tech.*, 2010, **3**, 375–386.
19. Karion, A. *et al.*, Long-term greenhouse gas measurements from aircraft. *Atmos. Meas. Techn.*, 2013, **6**, 511–526.
20. Suntharalingam, P. *et al.*, Improved quantification of Chinese carbon fluxes using CO₂/CO correlations in Asian outflow. *J. Geophys. Res.: Atmos.*, 2004, **109**; doi: 10.1029/2003JD004362.
21. Takegawa, N. *et al.*, Removal of NO_x and NO_y in Asian outflow plumes: aircraft measurements over the western Pacific in January 2002. *J. Geophys. Res.: Atmos.*, 2004, **109**; doi: 10.1029/2004JD004866.
22. Turnbull, J. C. *et al.*, Comparison of ¹⁴CO₂, CO, and SF₆ as tracers for recently added fossil fuel CO₂ in the atmosphere and implications for biological CO₂ exchange. *Geophys. Res. Lett.*, 2006, **33**; doi: 10.1029/2005GL024213.
23. Han, S. *et al.*, Temporal variations of elemental carbon in Beijing. *J. Geophys. Res.: Atmos.*, 2009, **114**; doi: 10.1029/2009JD012027.
24. Wang, Y. *et al.*, CO₂ and its correlation with CO at a rural site near Beijing: implications for combustion efficiency in China. *Atmos. Chem. Phys.*, 2010, **10**, 8881–8897.
25. Wunch, D. *et al.*, Emissions of greenhouse gases from a North American megacity. *Geophys. Res. Lett.*, 2009, **36**; doi: 10.1029/2009GL039825.
26. Wong, K. W. *et al.*, Mapping CH₄:CO₂ ratios in Los Angeles with CLARS-FTS from Mount Wilson, California. *Atmos. Chem. Phys.*, 2015, **15**, 241–252.

ACKNOWLEDGEMENTS. We thank PRL, Ahmedabad for encouragement and ISRO-GBP for financial support. We also thank P. K. Patra (JAMSTEC, Japan) for useful discussions; T. K. Sunilkumar (PRL) for help and S.L. thanks Tom Ryerson (NOAA, Boulder, USA) for useful suggestions about CO₂ measurements. We also thank the reviewer for useful comments and suggestions.

Received 2 June 2015; revised accepted 5 August 2015

doi: 10.18520/v109/i11/2111-2116

Observations of snow–meteorological parameters in Gangotri glacier region

H. S. Gusain*, Manish Kala, Ashwagosha Ganju, V. D. Mishra and Snehmami

Snow and Avalanche Study Establishment, Research and Development Centre, Chandigarh 160 036, India

In this communication analysis of the snow–meteorological parameters recorded in the Gangotri glacier region has been presented. Maximum temperature, minimum temperature, snowfall, snow cover thickness, incoming shortwave radiation flux, reflected shortwave radiation flux and albedo have been recorded at ‘Bhojbasra’ observation station. Meteorological data of 13 years from 2000 to 2012 have been presented for annual and seasonal variations in temperature, snowfall and snow cover thickness. Winter, pre-monsoon, monsoon and post-monsoon data have been considered for analysis. Annual mean maximum and minimum temperature are $11.1 \pm 0.7^\circ\text{C}$ and $-2.3 \pm 0.4^\circ\text{C}$ respectively. Mean values of these parameters obtained for winter season are $3.0 \pm 1.0^\circ\text{C}$ and $-10.4 \pm 1.3^\circ\text{C}$ respectively. Mean annual snowfall amount is 257.5 ± 81.6 cm and maximum snow cover thickness varies from 42 to 205 cm for different years. Incoming shortwave radiation flux and reflected shortwave radiation flux have been recorded using pyranometer sensor mounted on automatic weather station, and data for 2012 and 2013 are presented. Incoming shortwave radiation flux and total atmospheric transmissivity have been estimated. Mean annual atmospheric transmissivity is 0.37 at the observation location. Mean seasonal albedo for winter season is observed to be quite high compared to other seasons. Maximum and minimum temperature reveal an increase of 0.9°C and 0.05°C respectively, during the decade. Annual snowfall amount reveals a decrease of 37 cm in the decade. The observed temperature and snowfall patterns during the past 13 years, at the present study location, indicate that trends in Central Himalaya may be in accordance with the observed trends in the Western Himalaya.

Keywords: Albedo, glacier, snowfall, snow cover, temperature.

THE Himalaya Mountains are the abode of the largest number of glaciers outside the polar regions. These glaciers are the major source of many perennial river systems, including the Ganga, Indus and Brahmaputra¹. These rivers play a critical role in meeting the demands of water, irrigation and hydropower^{1,2}. Gangotri glacier is one of the most well-studied glaciers in India and is the largest glacier in the Garhwal Himalaya³. Studies of the Gangotri glacier have been conducted for analyses of glacier

*For correspondence. (e-mail: gusain_hs@yahoo.co.in)

retreat²⁻⁵, glacier dynamics^{4,6}, geomorphology, etc. However, very few studies have been presented on temporal variation in snow–meteorological parameters in the region⁷. Snow–meteorological parameters, e.g. air temperature, snowfall, snow cover thickness, wind, incoming shortwave radiation, etc. in the region have an impact on dynamics of the Gangotri glacier. The present communication reports the temporal variation of these snow–meteorological parameters in the region during different seasons using data of a little more than a decade.

Snow and meteorological parameters have been recorded manually at ‘Bhojbasa’ observation station (30°56′5.59″N, 79°4′26.41″E, ~3900 m amsl) about 5 km north-west from the Gangotri glacier snout named as ‘Gaumukh’ (Figure 1). Though the station is some distance away from the Gangotri glacier, it gives a fairly good idea about the snow and meteorological conditions in the region. At the observatory, the snow–meteorological parameters such as maximum temperature, minimum temperature, snowfall, snow cover thickness and wind speed are manually recorded daily throughout the year. These parameters for the period 2000–2012 have been analysed in the present study. Other parameters like incoming shortwave radiation, reflected shortwave radiation, etc. are recorded hourly using an Automatic Weather Station (AWS) at the same location and analysed for two years – 2012 and 2013.

The entire year was divided into four seasons, viz. winter (December, January, February), pre-monsoon (March, April, May), monsoon (June, July, August, September), and post-monsoon (October, November)^{8,9}. Monthly and seasonal averages for the parameters – maximum temperature, minimum temperature and snowfall were calculated from the data collected daily at the field observatory¹⁰. Total monthly snowfall was calculated by adding the daily fresh snowfall records. Monthly and seasonal averages of the incoming shortwave radiation flux and reflected shortwave radiation flux were calculated using hourly



Figure 1. A part of Gangotri glacier, snout position ‘Gaumukh’ and location of observation station ‘Bhojbasa’.

AWS data. Total seasonal and yearly atmospheric transmissivity was also estimated in the region. Incoming radiation at the top of the atmosphere at the observation location was calculated using solar zenith angle, mean Earth–Sun distance and solar constant¹¹. Solar zenith angle for each hour during 2012 and 2013 was estimated using digital elevation model of the region and ERDAS IMAGINE 9.3 software. Atmospheric transmissivity was calculated by estimating the ratio of observed incoming shortwave radiation at the observation location to incoming shortwave radiation at the top of the atmosphere.

Although we do not have long-term data (more than 30 years) to deduce climatic trends in the region, we have observed and analysed temperature and snowfall pattern during the last one decade.

Figure 2 *a* and *b* shows the temporal variation of yearly mean of maximum and minimum temperatures respectively in the study region. Maximum temperature varies from 9.8°C to 12°C with mean value of $11.1 \pm 0.7^\circ\text{C}$. The year 2004 is observed to be the warmest during the last decade. In seasonal variation of maximum temperature, monsoon season has the highest temperature with mean value of $17.1 \pm 0.8^\circ\text{C}$ followed by post-monsoon and pre-monsoon seasons with mean value of $11.3 \pm 1.0^\circ\text{C}$ and $12.2 \pm 1.4^\circ\text{C}$ respectively. As is obvious, maximum temperature for winter season is the lowest with mean value of $3.0 \pm 1.0^\circ\text{C}$. Minimum temperature varies from –1.5 to -2.9°C with mean value of $-2.3 \pm 0.4^\circ\text{C}$. Mean value of minimum temperature for winter, pre-monsoon, monsoon and post-monsoon seasons is $-10.4 \pm 1.3^\circ\text{C}$, $-3.2 \pm 0.8^\circ\text{C}$, $5.0 \pm 0.4^\circ\text{C}$ and $-3.6 \pm 0.9^\circ\text{C}$ respectively.

Highest values of maximum and minimum temperatures are observed for monsoon season as incoming solar radiation is observed to be highest during this season. High temperatures may cause higher melting rate of the glaciers in the region during this particular season. During winter season, incoming shortwave radiation flux is low and reflected shortwave radiation flux is high compared to the other seasons. This results in lower absorption of shortwave radiation flux at the surface and consequently low temperatures are obtained during this season.

During winter, snowfall in the region is mainly due to western disturbances (WDs). WDs are cyclonic storms associated with the mid-latitude subtropical westerly jet and are important synoptic weather systems producing extreme precipitation over northern India¹². Most of the annual snowfall received at the location is due to WDs. Figure 3 shows temporal variation of annual snowfall – from 137 to 416 cm with mean value of 257.5 ± 81.6 cm during the past 13 years. The year 2002 is observed to be one with the highest snowfall of 416 cm, while 2004 and 2009 are observed with least snowfall of 156 and 137 cm respectively. Snowfall events in the region are associated with the movement of WDs and their interaction with the local topography. Mean snowfall events per year in the region are observed to be 25 ± 6 events. Highest number

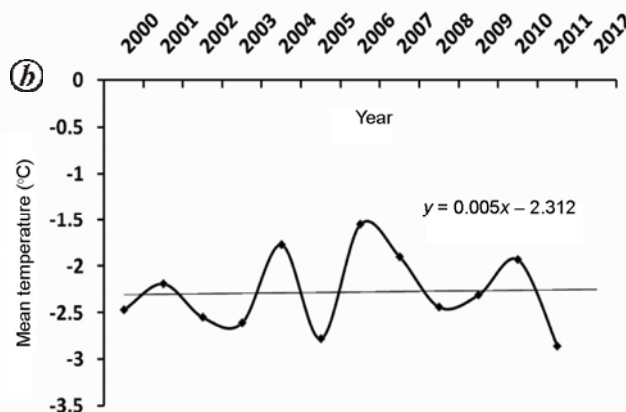
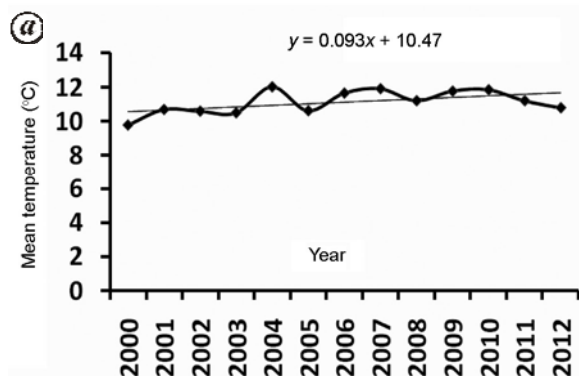


Figure 2. Temporal variation of yearly mean of (a) maximum temperature and (b) minimum temperature.

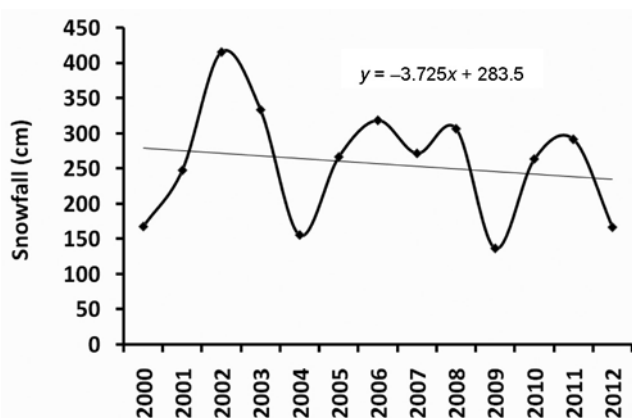


Figure 3. Temporal variation of annual snowfall.

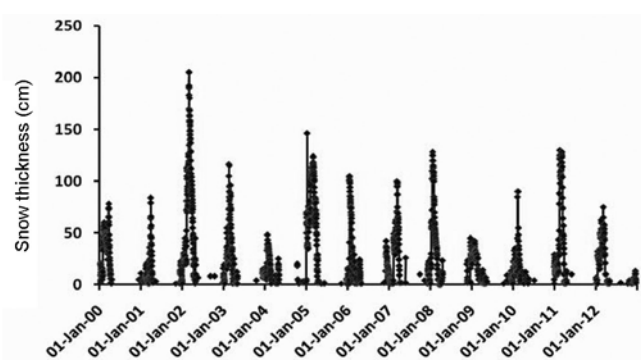


Figure 4. Temporal variation in snow cover thickness.

of 38 snowfall events is observed for 2002, resulting in highest snowfall during that year. Annual variation in snowfall in the present study location is mainly due to annual variation in the frequency and strength of the WDs, and their interaction with local topography. Strong WDs dissipate higher snowfall in the region compared to weak WDs. Dimri¹³ observed the connection between winter precipitation due to WDs in northwest India and

large-scale global forcing of El Niño Southern Oscillation (ENSO). He has reported a significant correlation between the two, indicating increased precipitation over northwest India during warm phases of ENSO and decreased precipitation during cold phases of ENSO. Years with least snowfall are observed to be comparatively warmer.

Figure 4 shows temporal variation in snow cover thickness at the observation location. Yearly cycle in snow cover thickness can be seen from the figure. Snow cover starts building up from November with the approach of WDs in the region and achieves maximum thickness during February/March. From then onwards, snow cover starts depleting due to rise in temperature and by June snow cover ablates completely. This cycle repeats every year; however the thickness varies from year to year depending upon the number of snowfall events (or the number of WD events), amount of snowfall (high snowfall during strong WDs and less snowfall during weak WDs), wind and radiation pattern, etc. Maximum snow cover thickness varies from 42 to 205 cm in the region during different years. Highest snow cover thickness of 205 cm has been recorded during 2002, for which highest snowfall and highest number of WD events have been observed. Years with least snowfall – 2004 and 2009 – also show minimum snow cover thicknesses of 48 and 42 cm respectively.

Annual mean wind speed in the region varies from 3.3 to 6.5 km/h, and 13 years' mean is 4.7 ± 0.8 km/h. Wind speed is observed to be high during winter season compared to monsoon. Mean annual values of cloud amount, which is observed daily at 08.30 and 17.30 h at the observation location, varies from 2.1 to 4.1 octa. Cloud cover plays an important role by blocking the transmission of incoming shortwave radiation flux from top of the atmosphere to the surface.

Figure 5 shows temporal variation in incoming shortwave radiation flux at the surface, incoming shortwave radiation flux at the top of the atmosphere above the observation location, and total atmospheric transmissivity

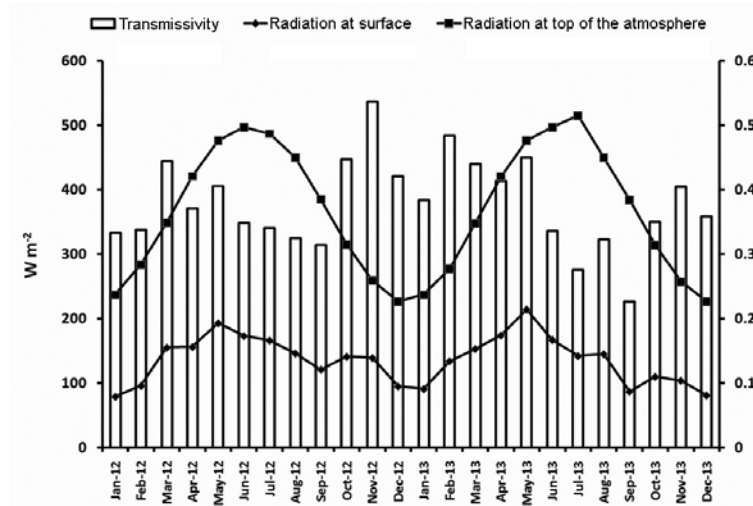


Figure 5. Temporal variation of incoming shortwave radiation flux (Wm^{-2}) at the surface, incoming shortwave radiation flux (Wm^{-2}) at the top of atmosphere and total atmospheric transmissivity (secondary axis).

for the years 2012 and 2013. Incoming shortwave radiation flux at the top of the atmosphere varies from 226 Wm^{-2} for December 2012 to 515 Wm^{-2} for July 2013 with annual mean value of 366 Wm^{-2} . Incoming shortwave radiation flux at the surface has been recorded using upward-looking pyranometer mounted on the AWS. Recorded flux at surface varies from 81 Wm^{-2} for December 2013 (monthly mean) to 214 Wm^{-2} for May 2013 (monthly mean) with annual mean of 136 Wm^{-2} . Total atmospheric transmissivity varies from 0.2 to 0.5 during different months with mean yearly transmissivity of 0.37. Atmospheric transmissivity depends on many factors, e.g. aerosols, atmospheric gases, water vapour, clouds, solar zenith angle, etc. Monthly variation in atmospheric transmissivity at the observation location is mainly due to variation in cloud cover during different months.

Atmospheric transmissivity during post-monsoon and pre-monsoon seasons is comparatively higher, probably due to less amount of cloud cover during these seasons. Although incoming shortwave radiation flux at the top of the atmosphere and at the surface are observed to be maximum during monsoon season, high absorption/reflection of shortwave radiation flux in the atmosphere due to cloud cover results in low atmospheric transmissivity during the monsoon season. High cloud cover during this season may also contribute to high attenuation of shortwave radiation flux in the atmosphere.

Mean monthly reflected shortwave radiation flux varies from 16 Wm^{-2} for September 2013 to 85 Wm^{-2} for February 2013. Yearly mean of reflected shortwave radiation flux is $39 \pm 18 \text{ Wm}^{-2}$. Reflected shortwave radiation flux for winter is higher compared to other seasons, as the surface is covered with snow during winter. AWS at the observation location is installed on bare ground and during seasons other than winter reflected shortwave radia-

tion flux is observed for soil surface. Seasonal mean albedo at the observation location varies from 0.2 during monsoon season to 0.6 during winter, and yearly mean albedo is observed to be 0.3. On the ice surface of the Gangotri glacier, the albedo will be higher compared to the observation location for all the seasons.

In the present communication, we have analysed data of 13 years from 2000 to 2012. Although we do not have long-term data (~ 30 years) to deduce the climatic trends, patterns in the snow-meteorological parameters during the past 13 years have been analysed. Analyses of maximum and minimum temperature data reveal a warming trend of 0.9 and $0.05^\circ\text{C}/\text{decade}$ respectively. A decreasing trend in the annual snowfall of 37 cm has been observed during the decade. The meteorological trends obtained have been tested for statistical significance using Mann-Kendall and Spearman t -test. The latter test reveals that the trends are statistically non-significant within 95% confidence limit while the former test shows no trends in the time series of the data. The increasing temperature trends and decreasing snowfall trends have also been observed at various observation locations of the Western Himalaya, and many researchers have reported these trends in the past¹⁴⁻¹⁶. Table 1 shows the trends in maximum temperature, minimum temperature and snowfall at a few observation stations of Pir Panjal and Great Himalayan ranges of the Western Himalaya. Gusain *et al.*¹⁵ have provided details of temperature and snowfall for 37 observation stations in the Western Himalaya and reported that most of the stations in Pir Panjal, Shamshabari and Great Himalayan range have increasing temperature and decreasing snowfall trends. The temperature and snowfall patterns observed during the past 13 years at the present study location (Bhojbas in Gangotri Glacier region) are indicative that trends in Central Himalaya may

Table 1. Trends in maximum temperature, minimum temperature and snowfall at few observation stations in the Western Himalaya

Observation station	Himalayan range	Maximum temperature	Minimum temperature	Snowfall
Manali	Pir Panjal	0.8°C/decade; increasing trend	0.5°C/decade; increasing trend	64 cm/decade; decreasing trend
Solang	Pir Panjal	0.8°C/decade; increasing trend	0.3°C/decade; increasing trend	35 cm/decade; decreasing trend
Gulmarg	Pir Panjal	0.9°C/decade; increasing trend	0.5°C/decade; increasing trend	27 cm/decade; decreasing trend
Patsio	Great Himalaya	1.0°C/decade; increasing trend	0.4°C/decade; increasing trend	79 cm/decade; decreasing trend
Kanzalwan (Gurej)	Great Himalaya	0.6°C/decade; increasing trend	0.09°C/decade; increasing trend	79 cm/decade; decreasing trend

be in accordance with the observed trends in the Western Himalaya.

The present communication analyses the annual and seasonal variation of various snow and meteorological parameters recorded at Bhojbasra observation station in the Gangotri glacier region. Annual mean of maximum temperature, minimum temperature, snowfall and wind are observed to be $11.1 \pm 0.7^\circ\text{C}$, $-2.3 \pm 0.4^\circ\text{C}$, 257.5 ± 81.6 cm and 4.7 ± 0.8 km/h respectively. The region is observed to be more windy during WDs compared to monsoon period. Annual variation has been observed in snowfall, and at the location of this study it depends on the frequency and strength of WDs and their interaction with local topography. Large temporal variation is observed in snow cover thickness; maximum snow cover thickness varies from 42 to 205 cm during different years. Annual mean incoming shortwave radiation flux at the top of atmosphere and the surface is 366 and 136 Wm^{-2} respectively. Total atmospheric transmissivity has been estimated from incoming shortwave radiation flux at the top of the atmosphere and at the surface. Mean atmospheric transmissivity is 0.37. Monthly variation in transmissivity is mainly due to variation in cloud cover. Mean albedo at the observation location during winter season is high compared to other seasons. Albedo values for the glacier surface will be higher compared to the observation location. Temperature in the region shows increasing trend and snowfall shows decreasing trend. Maximum temperature and minimum temperature reveal an increase of 0.9°C and 0.05°C respectively, during past decade. Annual snowfall amount reveals a decrease of 37 cm during the decade. These snow–meteorological parameters have a significant bearing on glacier accumulation/ablation pattern, and will influence glacier retreat and advancement. Seasonal variation of these parameters will lead to variation in glacier dynamics during the seasons.

1. Bolch, T. *et al.*, The state and fate of Himalayan glaciers. *Science*, 2012, **336**, 310–314.
2. Bahuguna, I. M. *et al.*, Are the Himalayan glaciers retreating? *Curr. Sci.*, 2014, **106**, 1008–1013.
3. Bhambri, R., Bolch, T. and Chaujar, R. K., Frontal recession of Gangotri Glacier, Garhwal Himalayas, from 1965 to 2006, measured through high-resolution remote sensing data. *Curr. Sci.*, 2012, **102**, 489–494.

4. Saraswat, P., Syed, T. H., Famiglietti, J. S., Fielding, E. J., Crippen, R. and Gupta, N., Recent changes in the snout position and surface velocity of Gangotri glacier observed from space. *Int. J. Remote Sensing*, 2013, **34:24**, 8653–8668.
5. Kulkarni, A. V. and Karyakarte, Y., Observed changes in Himalayan glaciers. *Curr. Sci.*, 2014, **106**, 237–244.
6. Gantayat, P., Kulkarni, A. V. and Srinivasan, J., Estimation of ice thickness using surface velocities and slope: case study at Gangotri Glacier India. *J. Glaciol.*, 2014, **60**, 277–282.
7. Negi, H. S., Thakur, N. K., Ganju, A. and Snehmami, Monitoring of Gangotri glacier using remote sensing and ground observations. *J. Earth Syst. Sci.*, 2012, **121**, 855–866.
8. Shrestha, A. B., Wake, C. P., Mayewski, P. A. and Dibb, J. E., Maximum temperature trends in the Himalaya and its vicinity: an analysis based on temperature records from Nepal for the period 1971–94. *J. Climate*, 1999, **12**, 2775–2786.
9. Dimri, A. P. and Dash, S. K., Winter temperature and precipitation trends in the Siachen Glacier. *Curr. Sci.*, 2010, **98**, 1620–1625.
10. Gusain, H. S., Chand, D., Thakur, N., Singh, A. and Ganju, A., Snow avalanche climatology of Indian Western Himalaya. In International Symposium on Snow and Avalanches, Manali, 6–10 April 2009.
11. Gusain, H. S., Mishra, V. D. and Arora, M. K., A four year record of the meteorological parameters, radiative and turbulent energy fluxes at the edge of the East Antarctic ice sheet, close to Schirmacher Oasis. *Antarctic Science*, 2014, **26**(1), 93–103.
12. Dimri, A. P., Niyogi, D., Barros, A. P., Ridley, J., Mohanty, U. C., Yasunari, T. and Sikka, D. R., Western disturbances: a review. *Rev. Geophys.*, 2015, **53**, doi:10.1002/2014RG000460.
13. Dimri, A. P., Relationship between ENSO phases with Northwest India winter precipitation. *Int. J. Climatol.*, 2012, doi:10.1002/joc.3559.
14. Dimri, A. P. and Dash, S. K., Winter climatic trends in the western Himalaya. *Climate Change*, 2012, **111**, 775–800.
15. Gusain, H. S., Mishra, V. D. and Bhutiyan, M. R., Winter temperature and snowfall trends in the cryospheric region of north-west Himalaya. *Mausam*, 2014, **65**(3), 425–432.
16. Shekhar, M., Chand, H., Kumar, S., Srinivasan, K. and Ganju, A., Climate change studies over western Himalayan region. *Ann. Glaciol.*, 2010, **51**, 105.

ACKNOWLEDGEMENT. We thank the staff of SASE, Chandigarh during collection of snow–meteorological data over the years, and the SASE Data Centre for providing data used in the present work.

Received 11 December 2014; revised accepted 13 August 2015

doi: 10.18520/v109/i11/2116-2120